

Charge Transfer and Chemisorption of Fullerene Molecules on Metal Surfaces: Application to Dynamics of Nanocars

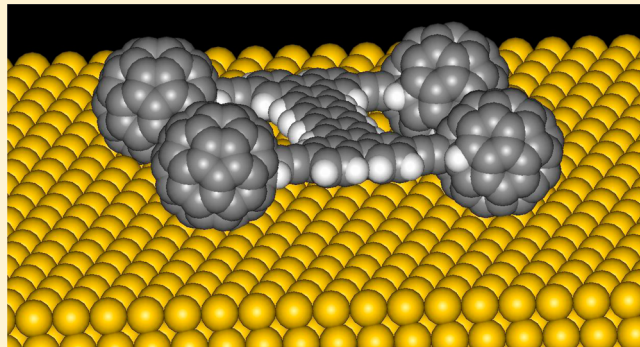
Alexey V. Akimov,^{*,†} Caitlin Williams,^{†,‡} and Anatoly B. Kolomeisky[†]

[†]Department of Chemistry, Rice University, 6100 Main Street, Houston, Texas 77005, United States

[‡]Department of Chemistry and Biochemistry, University of Arkansas, 119 Chemistry Building, Fayetteville, Arkansas 72701, United States

Supporting Information

ABSTRACT: It is widely believed that the dynamics of surface-bound fullerene molecules is not fully understood because current theoretical analyses do not include charge-transfer phenomena. A new theoretical approach to describe charge transfer and chemisorption processes for fullerenes on gold surfaces has been developed. The method is based on extensive semiempirical calculations that provide a consistent description of charge transfer and adsorption phenomena. Our theoretical approach is applied for analyzing complex dynamics of fullerene-based molecular machines, known as nanocars. It is found that the charge transfer makes the rolling of nanocars' wheels a preferable mode for translational motion because of the complex interactions with the metal surfaces. The physical-chemical aspects of the rolling mechanism are discussed.



1. INTRODUCTION

One of the most significant advances in recent nanoscale research was a creation of artificial molecular machines, known as nanocars.^{1,2} Such molecular objects are usually composed of the moderate size acene compounds and a few relatively spherical organic groups attached to them, mimicking the car's chassis and wheels correspondingly. Several wheel types have been utilized, including carboranes^{3,4} and organometallic complexes.⁵ However, the most popular choice for the molecular wheel is a fullerene (C_{60}) due to its high spherical symmetry and important physical/chemical properties. The direct observation of thermally induced motion of nanocars with C_{60} wheels in STM experiment⁶ has stimulated the development of various theoretical methods for understanding their mechanisms and dynamics.^{7,8} The most challenging part of these approaches is how to properly describe the interactions between the fullerene and the metal surfaces.

In our previous work,⁷ several specific models to predict these interactions have been considered. However, most of them treated the phenomenon of the charge transfer, which is known to be very important in C_{60} /metal systems,^{9–13} only via a parametrization of the dispersion interactions of Lennard-Jones or Morse type. These models, however, do not take into account the electrostatic nature of such interactions and substitute them with effective dispersion-type interactions. As a result, a correct quantitative dynamic description of nanocars on a gold surface has not been obtained, although the qualitative behavior has been matched reasonably well.⁷ The main problems of not accounting for the charge transfer are (1)

the much higher mobility of the nanocars as predicted theoretically in contrast to experimental observations and (2) the inability to describe their interactions with external electric fields.

Experimentally, the importance of taking into account electrostatic interactions has been demonstrated in recent works,^{6,14,15} where the STM tip was used as a source of strong electric field or as an excitation pump, capable of inducing either translational or rotational motion of molecular rotors and machines. Such motion cannot be predicted for nonpolar molecules without accounting for charge transfer phenomena.

The fullerene molecule has many unusual physical and chemical properties, and its interactions with different surfaces have been widely studied. So far, a variety of quantum mechanical calculations of interactions between C_{60} and diamond,¹⁶ graphite,¹⁷ silicon,¹⁸ silica and polyester¹⁹ surfaces as well as several studies of fullerene interactions with various metals such as gold,^{8,10,11,20–24} silver,^{10,25} copper,¹³ and several others^{26–28} have been performed. Recently also the DFT studies to understand the charge transfer and electronic structure in C_{60} /Au nanocontacts²⁹ as well as for C_{60} /Au interfaces³⁰ have been accomplished. However, most of these investigations utilize only static calculations of several fullerene/surface configurations, and typically they are too expensive to be used for realistic long-time dynamics simulations of complex

Received: April 12, 2012

Revised: June 5, 2012

Published: June 5, 2012



systems such as nanocars. Therefore, in order to better understand the dynamics of surface-moving molecular machines, it is essential to develop a computationally tractable approach, which still provides advantages of electronic structure calculation methods.

The most frequently used existing method to account for the charge transfer effects is a charge equilibration scheme (Qeq)³¹ and its different variations.^{32–35} Such an approach allows the calculation of charges of relatively large molecules as a function of positions of all atoms computationally much cheaper than it can be done with *ab initio* or semiempirical methods. However, the method works only for structures near their equilibrium. For example, it predicts ionic dissociation energies even for small molecules which are not observed in reality. Although some variations³⁶ of the original method allow us to solve this problem for small systems, there are many other inherent limitations of the Qeq method, which preclude its use for adsorbate–metal systems. First of all, for large molecules, the method becomes very expensive because of the necessity to solve large systems of linear equations. More importantly, the solution of such a system may become numerically unstable due to the almost linear dependency of the corresponding equations. Such calculations may converge to unphysical charge distribution or not converge at all. Finally, the Qeq method ignores quantum effects, which might lead to qualitatively incorrect charge distributions.

Despite the limitations of the Qeq method, it has been used in combination with other molecular mechanics methods for the number of adsorbates on various metal surfaces,^{23,37,38} including C₆₀ on gold.^{39,40} However, the predicted amount of charge, transferred from the metal to fullerene, calculated with such approaches is smaller than observed experimentally.²¹

Here we propose a new computational approach, based on fundamental physical considerations and semiempirical PM6 calculations,⁴¹ that is aimed to reproduce known experimental and/or high quality computational results related to C₆₀ adsorption on gold surfaces, while giving some mechanistic insight on the details of the charge transfer process and preserving the computational efficiency necessary for long molecular dynamics (MD) simulations of fullerene-based systems. The model is applied to study the surface diffusion of both fullerene and fullerene-based nanocars. We also show that the mechanism involving the rotation of the nanocar's wheels becomes a dominating factor for translational motion if the charge transfer between the fullerene groups and the gold surface is taken into account. This consistently explains other experimental observations available for the nanocar systems.

2. THEORETICAL MODEL

2.1. Model Definition. Most investigations of the adsorption of C₆₀ molecule on gold surfaces report a significant amount of charge transfer (CT) from the metal to the fullerene, which may also depend on the structure of the specific crystal plane. Experimental studies show very different results with a significant uncertainty in measured values. For example, CT is estimated to be 0.8 electrons on the Au(111) surface,²¹ 1.0 ± 1.0 on the Au(110) surface^{10,11} (vibrational spectroscopy), and 1.0 ± 0.2 on polycrystalline Au⁹ (XPS with K-doping), while the theoretical model predicts that the CT is between 0.2–0.4 electrons on Au surfaces.^{39,42} It has been argued that the charge transfer is smaller for more open surfaces such as Au(111) or Au(100) in contrast to more corrugated surfaces such as Au(110).¹¹

The adsorption energy of C₆₀ on Au(111) was studied by both experimental and theoretical methods. Using the temperature desorption technique, it was estimated to be ~43 kcal/mol,²¹ whereas the DFT calculations²⁵ predict a somewhat lower value of only ~31 kcal/mol. The theoretical model in ref 23 gives the estimate for the adsorption energy on the Au(110) surface from 46 to 71 kcal/mol, depending on the proposed substrate structure (not taking into account the relaxation). It is argued that the adsorption energy on the reconstructed Au(110) surface is stronger than that on the Au(111) surface, which almost does not reconstruct after the C₆₀ binding.²¹

In our theoretical approach, we use the semiempirical PM6 calculations of the fullerene–gold systems for computing the charges on carbon atoms of the fullerene that depend on their distances to the metal surface. Consequently, the obtained data are used to fit the computationally more tractable model, which allows us then to do fast calculations of the charge distribution on the fullerene as well as its interaction energy with the metal surface. Since the charge distribution not only depends on the carbon–surface distance but also is a function of the orientation of carbon atoms with respect to each other and to the surface atoms, the calculations should be performed for many configurations. Although DFT studies of similar systems have been reported,^{12,25,27} they are usually performed for only a few points. Thus, for our purposes, only the semiempirical calculations would be practical.

One of the most popular semiempirical methods utilized for studying different processes on metal surfaces^{43–45} is the extended Huckel^{46–49} method. This method was originally designed for organic compounds, and it was later parametrized for transition metals in a way that also partially accounts for relativistic effects.^{50–52} However, in our preliminary studies, we have found that the convergence of such calculations for certain *d*-metals (including gold) was very problematic. It suggested to us to try another recently developed semiempirical method, parametrized for most elements in the periodic table, including transition metals, namely, the PM6 model.⁴¹ In addition, unlike the very approximate construction of the (extended) Huckel method,^{43,44,46–51} the PM6 method is based on less dramatic approximations, which gives it more flexibility for a better description of many systems.

Before using the PM6 method, we checked its quality by calculating the work function of the fullerene and several gold clusters (see Supporting Information section S1). As it follows from our calculations, the work function of the gold surface is overestimated by the PM6 method by a factor of 1.5–2.0 for small clusters and by a factor of 3 for bigger clusters. We also observed the overestimation of the work function of fullerene by a factor of ~1.4. Thus, if relatively small metal clusters are used, the qualitative picture should remain correct because the relative electron attraction strength will remain similar to experimental estimates.

The PM6 semiempirical calculations have been performed using the Gaussian 09⁵³ program package. Our preliminary results of the C₆₀/Au(100) system show that the charge transfer takes place only for small fullerene–gold distances. As a result, the carbon atom which is closest to any of the gold atoms becomes positively charged (0.3–0.4 au). Three adjacent carbon atoms which are directly connected to it become negatively charged (~−0.6 to −0.7 au). The charge transfer involving other carbon atoms is less significant (Figure 1), and the rest of the fullerene carbons carry significantly smaller partial charge, decreasing in absolute value from the bottom to

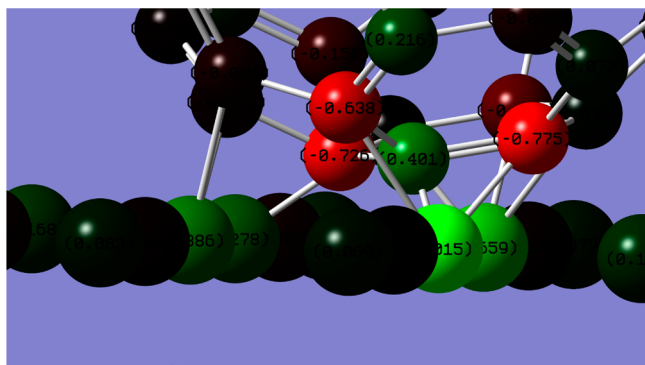


Figure 1. Typical charge transfer pattern in the $C_{60}/\text{Au}(100)$ system.

the top of the fullerene. Such observations reveal the very local nature of the charge transfer in the fullerene–gold system. The charges on gold atoms are not of particular interest because they do not have physical meaning. In reality, the charges in the metal are smeared and one should use electron density instead. Moreover, for construction of the surface–molecule interaction potential, we use only the charges of the adsorbate and assume the corresponding image charges in the metal.

In this work, we developed a relatively simple and physically intuitive approach to model the charge transfer of such kind, allowing us to perform fast calculations during the MD simulations of nanocar motion on gold surfaces. Moreover, since our goal is to run the efficient MD simulations, the developed approach is designed to be continuous, meaning that one should be able to calculate the derivatives of the charges on all atoms (of C_{60}) with respect to the positions of all atoms (themselves and others).

Since the shortest C–Au distance defines the most important positively charged carbon atoms, it is reasonable to define a continuous weight function that changes fast for a small distance difference. Using analogy with the continuous representation of delta-function as well as trying to mimic the exponential decay of the electron density with increasing distance to the closest atom, we can write down the total “electron density” on given carbon atom i due to its neighboring metal atoms as

$$\rho_i = \sum_{k \in \text{Au}} e^{-\alpha r_{ik}} S_1(r_{ik}) \quad (1)$$

where α is a model parameter and $S_1(r)$ is a switching function designed for better efficiency of calculations (in order to not consider all atoms of the surface). The switching function may in principle be chosen as any sufficiently smooth function (up to at least first derivatives). In this work, we use the switching function of the following kind:

$$S(r|R_{\text{on}}, R_{\text{off}}) = \begin{cases} 1 & r < R_{\text{on}} \\ \left(\frac{R_{\text{off}} - r}{R_{\text{off}} - R_{\text{on}}}\right)^3 \left(1 + 3 \frac{r - R_{\text{on}}}{R_{\text{off}} - R_{\text{on}}} + 6 \left(\frac{r - R_{\text{on}}}{R_{\text{off}} - R_{\text{on}}}\right)^2\right) & R_{\text{on}} \leq r \leq R_{\text{off}} \\ 0 & r > R_{\text{off}} \end{cases} \quad (2)$$

where R_{on} and R_{off} are model parameters.

Now, to describe the positive charge on the carbon atom with the shortest distance to one of the Au atoms, it is reasonable to assume some linear relation:

$$\begin{aligned} q_i &= \beta \rho_i \\ \beta &> 0 \end{aligned} \quad (3)$$

However, this would result in all carbon atoms being positively charged. So we need some extra term describing negatively charged carbon atoms. Here we make the use of the following observation. The biggest negative charges are observed on the atoms closest to the most important positively charged carbon. So the expression (3) will be modified as follows

$$\begin{aligned} q_i &= \beta \rho_i - \gamma \sum_{\substack{j \neq i \\ j \in C}} \rho_j S_2(r_{ij}) \\ \beta &> 0 \\ \gamma &> 0 \end{aligned} \quad (4)$$

where $S_2(r)$ is another switching function, of the same functional form, but with different parameters R_{on} and R_{off} . This switching function is necessary to model the charge back-donation only from the closest carbon atoms. Equations 1 and 4 constitute our charge transfer model. It is important to point out the important asymptotic property of the model. Namely, that the charge transfer amount is zero for large enough C_{60} –surface separation distances; i.e., the pure fullerene is neutrally charged, which is not the case for the charge equilibration scheme.³¹ The computational efficiency of the model is achieved by using the switching function S_1 which allows one to consider quite a few metal atoms per each of the bottom carbon atoms of the fullerene molecule. The atoms on the top may even not be involved in charge transfer processes at all.

The charges on carbon atoms of fullerene are calculated via (4) and then utilized in the potential of the form

$$\begin{aligned} E &= E_{\text{vdw}} + E_{\text{elec}} \\ E_{\text{elec}} &= \sum_{i \in \text{real}} \left(\chi_i q_i + \frac{1}{2} J_i q_i^2 + q_i \sum_{\substack{j \in \text{real} \\ j \neq i}} \frac{q_j}{r_{ij}} + q_i \sum_{j \in \text{image}} \frac{\tilde{q}_j}{\tilde{r}_{ij}} \right) \\ E_{\text{vdw}} &= D \left[\left(\frac{\sigma_{\text{C-Au}}}{r} \right)^{12} - 2 \left(\frac{\sigma_{\text{C-Au}}}{r} \right)^6 \right] \end{aligned} \quad (5)$$

where the quantities \tilde{q}_i and \tilde{r}_{ij} are the image charge of the particle i and the distance between the particle i and the position of the image of the particle j correspondingly.

Most of the parameters for the chemisorption model (5) are taken from different literature sources, namely, $\chi_C = 5.343$ eV, $J_C = 10.126$ eV,³¹ and $D_{C-Au} = 0.064$ kcal/mol.⁵⁴ However, we optimized the parameter σ_{C-Au} in such a way that it reproduces the experimentally observed amount of charge transfer on both Au(111) and Au(100) surfaces as well as the adsorption energies on corresponding surfaces.^{11,21} We found that the reported⁵⁵ value of $\sigma_{C-Au} = 2.74$ Å gives a reasonable approximation for average surface–molecule interaction energies as well as for the average charge transfer amounts. It is also close to a value of 2.9943 Å used in other similar studies.^{56–58}

2.2. Data Generation. As found in our preliminary calculations, a significant charge transfer happens in the very local regions of the fullerene/gold interface. For practical purposes, this means that the size of the gold slab might be decreased without a significant loss in the accuracy of calculated charges. We have tried several sizes of the gold slab with the same relative orientation and position (both set arbitrarily) of the fullerene molecule and the gold surface. Calculated charges for most important four carbon atoms are summarized in Table 1.

Table 1. Charges on the Four Most Important Atoms Calculated with Different Slab Sizes

atoms	$7 \times 7 \times 4$	$7 \times 7 \times 2$	$4 \times 4 \times 2$
C(positive)	0.400668	0.327544	0.314259
C(negative)	-0.637847	-0.670341	-0.546218
	-0.726158	-0.619585	-0.777108
	-0.775201	-0.781237	-0.719942
CPU time	3 h	1 h	1 min

Although the system size $4 \times 4 \times 2$ seems to be computationally the most efficient among those 3, we decided to slightly increase the lateral dimensions to 5×6 size, so for each translation in [0, 2.035] range both closest atoms and their immediate neighbors have a similar environment of gold atoms.

We performed a series of PM6 single point energy calculations for different configurations of the $C_{60}/Au(100)$ and $C_{60}/Au(111)$ systems. Such configurations were obtained by translating the fullerene molecule in x , y , and z directions (assuming the z direction is normal to the surface). For the $C_{60}/Au(100)$ system, the orientations of the fullerene with respect to the gold were chosen in the following way: the one where the edge joining 5 and 6 member rings is parallel to the surface plane and the other one is where the joining of two 6-member rings is parallel to the surface. For the $C_{60}/Au(111)$ system, we considered two other types of C_{60} orientations, one where the 5-member ring and another one with the 6-membered ring is parallel to the gold surface. For each orientation, we calculated approximately 175 points, different by the amount of the translation in x , y , and z directions. The systems used for calculations as well as the range of their x and y translations are presented in Figure 2. The number of metal atoms in gold clusters (representing the surfaces) was 30 for the Au(100) surface and 88 for the Au(111) surface correspondingly.

2.3. Fitting Model Parameters. As discussed earlier, in order to use our model, the set of parameters α , β , γ , $R_{on,1}$, $R_{off,1}$,

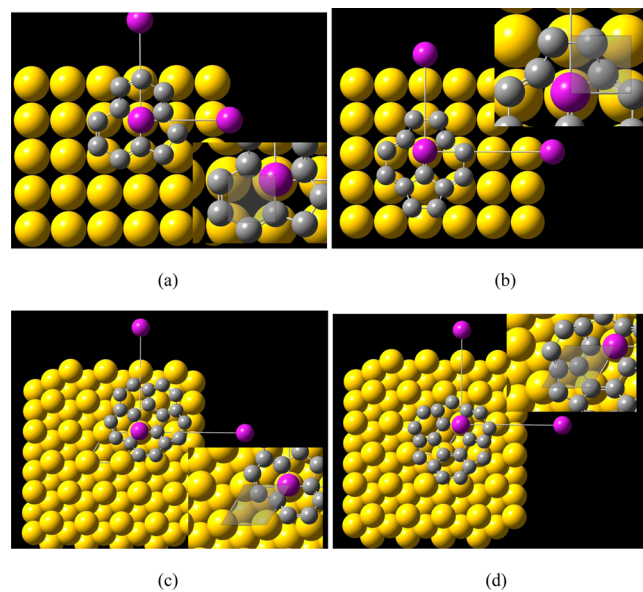


Figure 2. The systems used for calculations (only bottom atoms of C_{60} are shown for clarity) and the range of translations of the atom shown in purple. The systems differ by the orientation of the fullerene bottom with respect to the surface: (a) C_{60} oriented by the edge joining 5 and 6 member rings parallel to the Au(100) surface, (b) C_{60} oriented by the edge joining two 6 member rings parallel to the Au(100) surface, (c) C_{60} oriented by pentagon parallel to the Au(111) surface, (d) C_{60} oriented by hexagon parallel to the Au(111) surface.

$R_{on,2}$, and $R_{off,2}$ should be found which allows simultaneous calculation of the most important charges for all configurations. We used a steepest descent optimization algorithm to fit the model to calculated charges. However, we fitted only α , β , and γ parameters. The rest of the parameters were predetermined from the physical nature of the phenomenon. The quantity $R_{off,1}$ determines the range of C–Au separation distances where the charge transfer is still significant. Moreover, at C–Au distances larger than the equilibrium van der Waals (vdw) distance, the charge transfer effect should be negligible and we should be able to describe interactions with only vdw terms. Since the vdw equilibrium distance was chosen to be 2.74 Å, we set $R_{off,1} = 3.0$ Å. The quantity $R_{on,1}$ was empirically set to 0.0 Å, since this quantity helped to decrease the fitting error.

Another observation and assumption of the model is that the effect of first neighbors in C–C charge flow is dominating. Thus, it is unnecessary to choose parameter $R_{off,2}$ to be significantly larger than the C–C covalent distance. Because of that, it was set to a value of 2.0 Å. Similarly, the parameter $R_{on,2}$ was empirically set to 1.5 Å.

The accuracy of fitting was monitored by the average squared error quantity:

$$MSE = \frac{1}{N} \sum_{c=1}^N \sum_{i=1}^{60} (q_{c,i}^{\text{model}} - q_{c,i}^{\text{PM6}})^2 \quad (6)$$

where N is the number of configurations (~ 700) and $q_{c,i}^{\text{model}}$ and $q_{c,i}^{\text{PM6}}$ are the charges on the i th carbon atom of the c th configurations calculated by the model or taken from PM6 calculations correspondingly.

We have achieved the value of $MSE = 0.391$ in our fitting procedure, which gives quite a reasonable description of charges. It should be noted that this value of MSE is a most conservative measure for the accuracy, since it also takes into

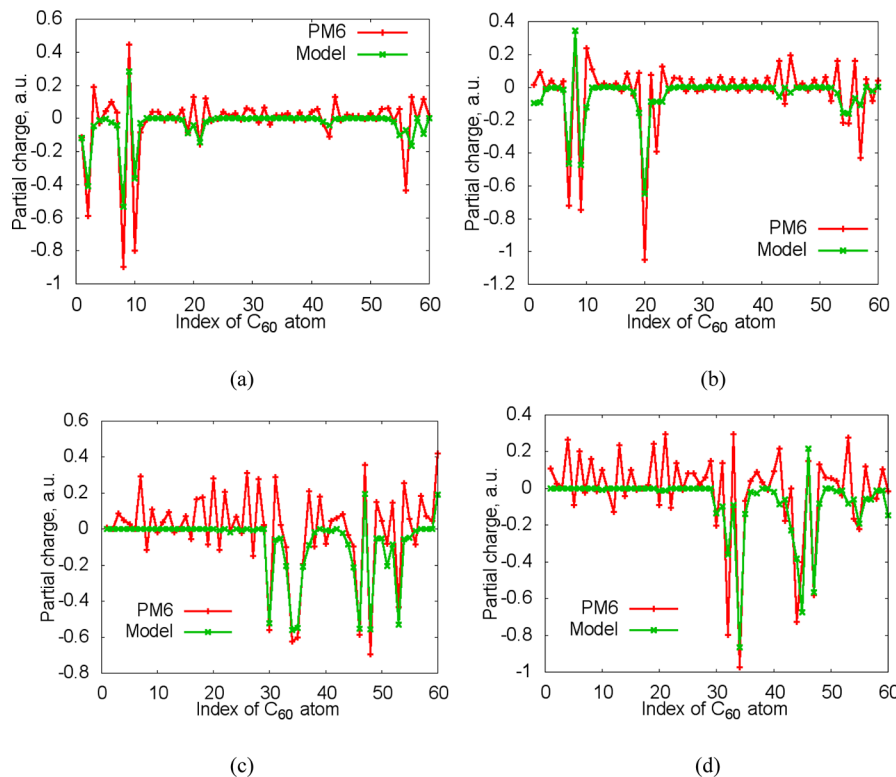


Figure 3. Charges on all carbon atoms for some of the configurations tested: (a) in the orientation of fullerene, where the 5,6 edge is toward the Au(100) surface; (b) the orientation where the 6,6 edge is toward the Au(100) surface; (c) the orientation where the 6-membered ring is parallel to the Au(111) surface; (d) the orientation where the 5-membered ring is parallel to the Au(111) surface. Configurations correspond to those shown in Figure 2.

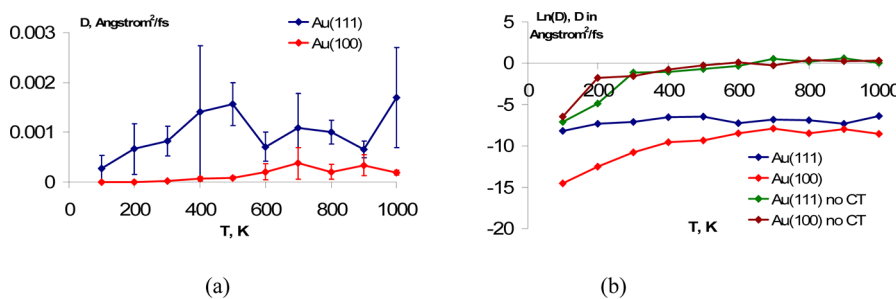


Figure 4. (a) Diffusion coefficients of C₆₀ on both Au(111) and Au(100) surfaces; (b) comparison with the system with only van der Waals interactions.

account those charges which do not participate in the training procedure, and because the cut-offs used in the model predicting the charges are set to zero, while the actual PM6 charges are not. Using only those charges that are actually involved in the training process would only decrease the MSE quantity.

The final values of the optimized parameters are: $\alpha = 1.91948847656 \text{ Å}^{-1}$, $\beta = 10.1435003541$, and $\gamma = 7.89007128485$. The approximate results for charges on all 60 carbon atoms for some randomly chosen configurations are shown in Figure 3.

As the figures suggest, the model gives quite reasonable predictions of the charges on the most important four carbon atoms. Moreover, in some cases, the minor charges are also predicted well. Obviously, the model is too simple to describe well all the charges. In order to improve on our approximation, one may choose to use several exponents in eq 1, perhaps with some linear scaling coefficients. Equation 1 may be interpreted

as a single-term representation of the electron density at a given spatial point. Using more than one term would mimic the MO LCAO method, however, without solving the corresponding secular equations.

3. RESULTS AND DISCUSSION

3.1. MD Simulation of C₆₀ on Au(111) and Au(100) Surfaces. We performed rigid-body MD simulations of a single C₆₀ molecule on a quasi-infinite gold surface at series of temperatures in the range 100–1000 K. To maintain the temperature constant, the Nosé–Hoover chain thermostat was used in combination with the rigid-body quaternion integration scheme of Kamberaj–Low–Neal.⁵⁹ For each temperature, five trajectories (2.5 ns long each) were sampled using an integration time step of 1 fs. Diffusion coefficients were calculated for each temperature using the formula

$$\langle dx^2 + dy^2 \rangle = 4Dt \quad (7)$$

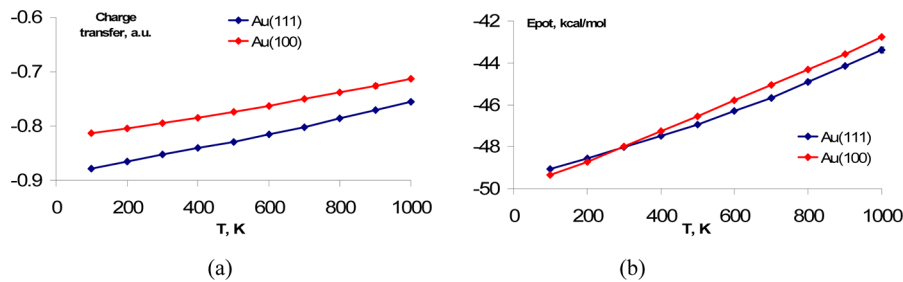


Figure 5. Average charge transfer amount (a) and the adsorption energy (b) for C₆₀ molecule on Au(111) and Au(100) surfaces.

The activation energy for diffusion on each surface was estimated using the Arrhenius equation

$$D(T) = D_0 e^{-E_a/k_B T} \quad (8)$$

where D_0 is a diffusion constant for the case when there are no molecule–surface interactions (free diffusion).

The activation energies for fullerene diffusion on Au(111) and Au(100) surfaces were found to be 0.30 and 1.49 kcal/mol, respectively. This may be interpreted as Au(111) being flatter decreases the activation energies for diffusion. This leads to diffusion coefficients on the Au(111) surface being higher in comparison to the diffusion coefficients on the Au(100) surface (see Figure 4).

We also calculated the average charge transfer amounts and the surface–molecule interaction energy, which in our case is identical to the adsorption energy. The charge transfer amount is larger in absolute value for the Au(111) surface plane (Figure 5a), while the adsorption energies are similar for both surfaces. This is a consequence of the higher number density of gold atoms per unit area on the Au(111) surface.

The average amount of charge transferred per C₆₀ molecule varies in the range of -0.9 to -0.7 electrons, which is in good agreement with the experimental findings²¹ but is larger (in absolute value) than the amount obtained with models based on the Qeq scheme³⁹ as well as from the corresponding DFT calculations.⁴² It should be noted, however, that these DFT calculations use the supercells with C₆₀ forming a monolayer; thus, the charge transfer is smaller in comparison to what one would obtain for the single fullerene molecule adsorbed on the gold surface. The average surface–molecule interaction energy is slightly higher than the experimentally measured value of ~43 kcal/mol; however, it agrees well with the value reported in other MD studies.³⁹ The difference with experimental result might be explained by the fact that the value of 43 kcal/mol was obtained for the desorption energy from the monolayer, not for a single fullerene. It is also known that the coadsorption phenomena^{60–62} usually results in weaker interactions between adsorbate and the surface. To account for this effect, we choose the σ_{C-Au} parameter such that the adsorption energy of a single molecule was larger than that reported for the monolayer.

In order to evaluate the importance of the charge transfer, we performed similar simulations taking into account only vdw interactions between the molecule and the surface. As expected, the difference in the diffusion coefficients was significant, reaching several orders of magnitude (Figure 4b). The average surface–molecule interaction energy was found to be comparable to the thermal energy $k_B T$ for temperatures as low as 100–200 K, indicating that only vdw interactions are not enough to describe strong binding of the fullerene molecules on metal surfaces. This also prohibited the use of Arrhenius

relation 8 for estimation of the activation energies for diffusion, which are apparently very small in this case.

3.2. MD Simulation of Nanotruck Molecule on Au(111) and Au(100) Surfaces. We also performed a series of MD simulations of the nanotruck molecule¹ which contains four fullerene groups attached to one common chassis group and functioning as wheels (Figure 6). In addition to the charge-

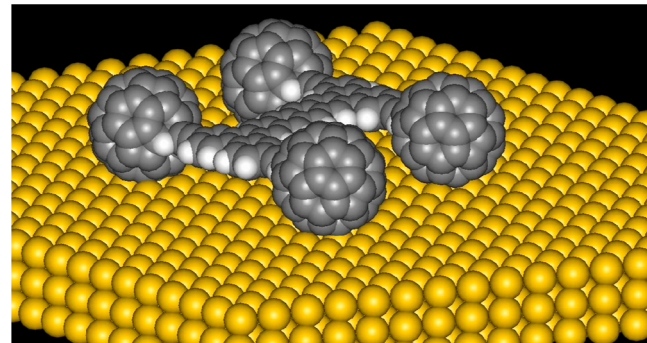


Figure 6. Nanotruck molecule on the gold surface.

transfer potential, eq 5, the universal force field (UFF)⁵⁴ has been used to describe the intramolecular interactions between the parts of the nanotruck molecule as well as the van der Waals interactions between the chassis part of the nanotruck and the metal surface. Since the gold surface is represented as a single rigid body, we do not use any interaction potential for the gold atoms in a metal. For each temperature, five trajectories (250 ps long each) were sampled using an integration time step of 1 fs. In order to improve sampling quality, we extended the temperature range over which simulations were performed to 100–2000 K.

Because of the geometric constraints, the fullerene groups in the nanotruck molecule closely resemble the monolayer of C₆₀ molecules. Therefore, we should expect some coadsorption effects taking place in this system. The average C₆₀–surface interaction energy as well as the charge transfer amount per C₆₀ molecule are presented in Figure 7. The average adsorption energies are indeed smaller than those for individual fullerene molecules and are comparable to the experimental value for the C₆₀ monolayer (43 kcal/mol). The charge transfer amount is also smaller than that for the single C₆₀ molecule, but it is still in good agreement with experimental values.

The mobility of the nanotrucks is 1–2 orders of magnitude smaller than that of the single fullerene molecules (Figure 8a). Similarly to the C₆₀/Au system, the diffusion coefficients calculated without charge transfer effects taken into account were several orders of magnitude higher (Figure 8b). For comparison, the diffusion coefficients of similar molecules,

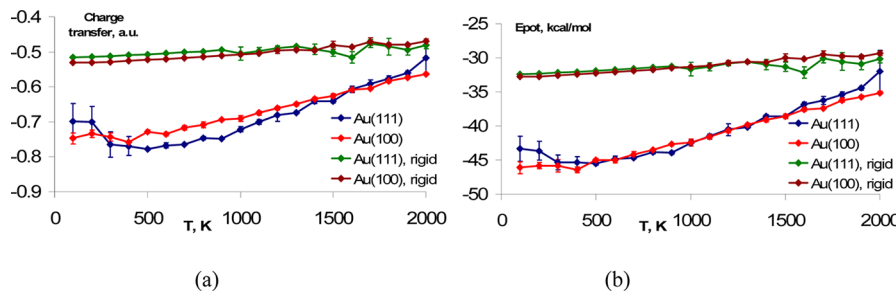


Figure 7. Average charge transfer amount (a) and the surface–molecule interaction energy (b) for nanotruck molecule per fullerene group calculated for flexible and rigid nanocars on both Au(111) and Au(100) surfaces.

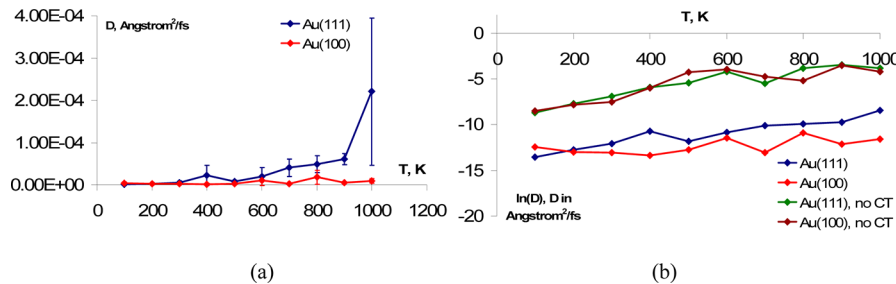


Figure 8. Diffusion coefficients of the nanotruck (with rotating “wheels”) on both Au(111) and Au(100) surfaces.

determined experimentally, vary in the range of 10^{-13} – 10^{-10} Å²/fs,^{6,63–65} while the molecular interaction models, which neglect the effect of the charge transfer, yield diffusion coefficients of the order of 10^{-2} Å²/fs. For the range of temperatures of 100–500 K, our charge transfer model predicts the diffusion coefficients of the order of 10^{-6} Å²/fs—a significant improvement toward the experimental values. We should note, however, that our model neglects almost all internal vibrations of the nanocar molecule as well as those of the metal substrate. This is known to affect the computed dynamical properties, by increasing them by several orders of magnitude because of the excess entropy associated with the coarse-graining.^{66–69}

The estimated activation energies for diffusion of the flexible nanocar molecule on the Au(111) and Au(100) surfaces are 4.0 ± 0.6 and 6.7 ± 1.0 kcal/mol correspondingly. Without the charge transfer effects, the activation energies are lower, 2.1 ± 0.3 and 2.7 ± 0.7 kcal/mol, respectively.

3.3. Importance of Wheels’ Rotations. In order to assess the importance of the wheels’ rotation on the mobility of the nanotruck, we performed rigid-body-MD simulation with all C₆₀ fragments and the chassis moiety combined into a single rigid body. In other words, in this case, we have imposed the artificial constraints that prevent fullerene wheels from rotation. We performed such calculations for both Au(111) and Au(100) surfaces. The comparison with the model, in which fullerene rotations are allowed, is presented in Figure 9. In both cases, the diffusion on the Au(111) surface is much faster than that on Au(100) for the same reason as we discussed above.

The diffusion coefficients for the rigid nanocars, where the rotation of the wheels is prohibited and the only way to move is via sliding or hopping, is by 1–2 orders of magnitude smaller than that for the 5-fragment nanocars with rotating fullerene wheels. Additional examination of the charge transfer amounts in both cases as well as corresponding average surface–molecule interaction energies (Figure 7) show that both of these quantities are smaller for the rigid molecule.

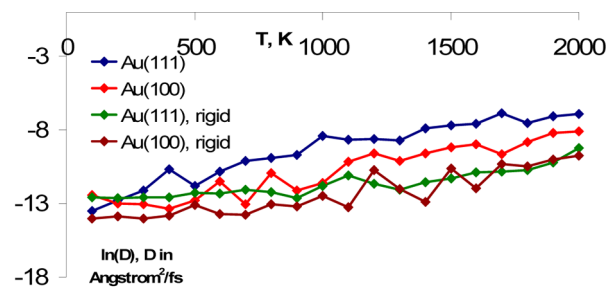


Figure 9. Comparison on the diffusion coefficients (logarithmic scale) for 5-fragment (flexible) and 1-fragment (rigid) nanocars on both Au(111) and Au(100) surfaces.

Intuitively, smaller charge transfer amount for the rigid molecules and smaller surface–molecule interaction energy suggest faster diffusion of the rigid molecules in contrast to nanocars with flexible wheels capable of rotating. However, this is in contrast to the calculated diffusion coefficients, as shown in Figure 9. This observation indicates that the rotation of the fullerene wheels significantly influences the mechanism of diffusion. Under these conditions, fullerene rolling is one of the main contributions to the overall mobility of nanotrucks on gold surfaces.

This finding may be explained in terms of energy diagrams for diffusion and desorption.^{70,71} The surface–molecule interaction energy determines the processes of adsorption–desorption of the ad-molecules as well as the processes involving motion of the molecules in the direction normal to the surface, such as jumps. Thus, the surface–molecule interaction energy itself does not determine the activation barriers for diffusion and consequently the diffusion coefficients. During the rolling motion of fullerene wheels, all atoms in a nanotruck do not move significantly in the vertical direction, thus decreasing the activation barrier and increasing the diffusion coefficients. It should be noted that certain correlations between the activation energies for diffusion and

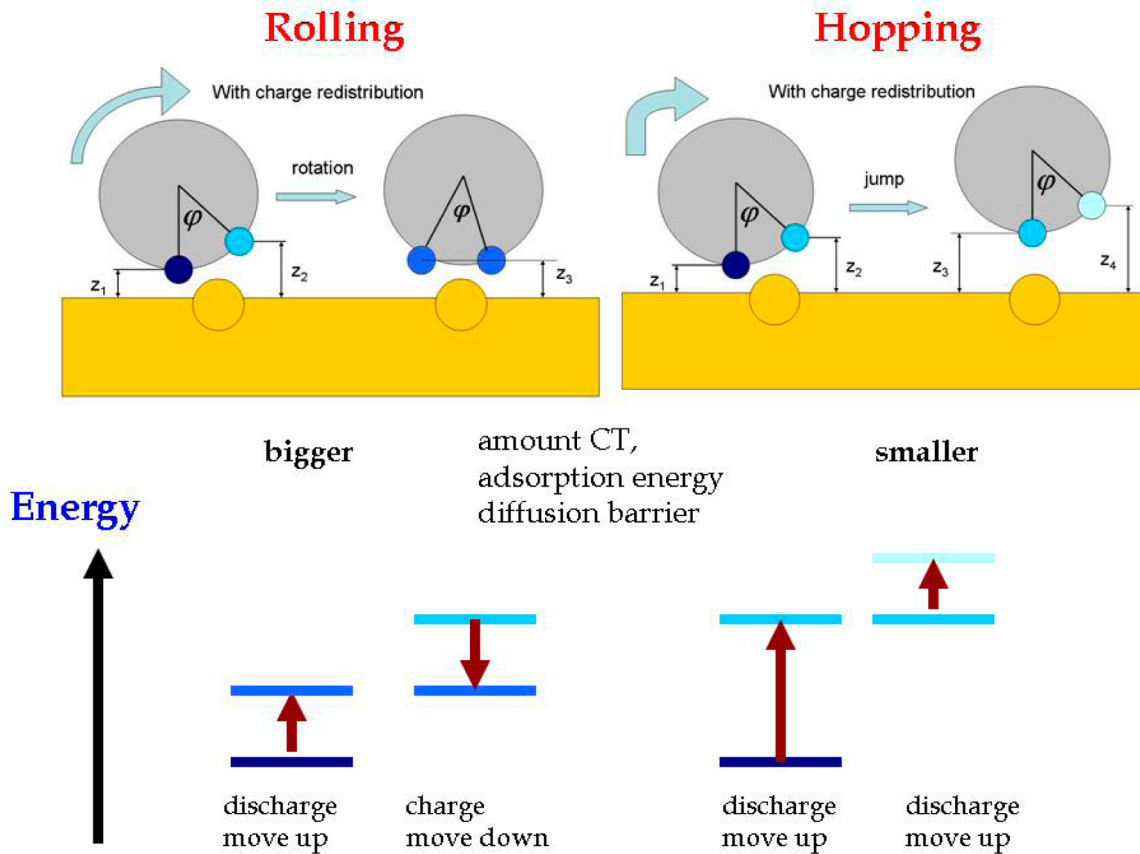


Figure 10. The explanation of the effect of the charge transfer on the diffusion (rolling vs hopping) mechanism of nanomachines. Two possible mechanisms are compared: rolling vs hopping. For rolling, $z_1 < z_3 < z_2$. For hopping, $z_1 < z_3$ and $z_2 < z_4$.

surface–adsorbate interaction energies have been reported for *n*-alkane molecules^{72–74} or their isomers,⁷⁵ which suggest that stronger surface–molecule interactions should slow down the lateral diffusion. However, in contrast to alkane systems where all parts of the molecule are almost equally distant from the surface at all times and the charge transfer effects are almost negligible, the atoms of the nanotruck’s wheel are at different distances from the surface and the charge transfer is substantial. However, the most important argument is that the nanocar’s surface diffusion involves mostly the rolling motion of its wheels which is impossible for *n*-alkanes. All of these factors lead to a very weak correlation between the surface adsorption and surface diffusion energies for the nanotruck, as observed in our calculations.

It turns out that when one prohibits the internal rotation of the fullerene wheels in the nanocar molecule, the mechanism for diffusion changes drastically (Figure 10). The charge transfer process is the important factor of the nanocar motion which is tightly related to the mechanism of diffusion.

Figure 9 compares two possible types of behavior of the fullerene “wheel” during the motion of the nanocar, namely, rolling and hopping. For simplicity, we focused only on two carbon atoms of the C₆₀ fragment on its bottom. The bottom part of Figure 10 schematically shows how the energy contributions due to these marked atoms change along the reaction coordinates. For each mechanism, the energy cost associated with the transition between the reactant (left) and the transition (right) states can be calculated as a sum of atomic contributions. The resulting sum specifies the activation barrier for each process. The initial and final positions and the charges

of each carbon atom determine whether the system gains or loses some energy.

For a conceptual simplicity, we consider only the energy change due to the charge–image interactions and neglect self- and intramolecular interactions in eq 5. Also the energy change due to vdw interaction will be omitted, since it very weakly depends on the charge transfer process. With these assumptions, the energy change due to the motion of atom *i* can be written as

$$\Delta E = E_{TS} - E_{reactant} = \left(-\frac{q^2(z_{TS})}{2z_{TS}} \right) - \left(-\frac{q^2(z_{react})}{2z_{react}} \right) \quad (9)$$

When an atom moves away from the surface, the total energy of the resulting state increases because of two reasons: (a) the distance between the atom and its image increases (on Figure 10 denoted as move up); (b) the atom loses negative charge (on Figure 10 denoted discharge). On the contrary, when the atom moves toward the surface, the energy of the system lowers by the same reasons (only acting in the opposite direction). Let us now compare rolling and sliding mechanisms from this schematic energy diagram. For simplicity, we only consider the atomic contribution to the total energy of state, due to two bottom atoms of fullerene, as shown in Figure 10. This however will not affect the general conclusions, because for other atoms similar derivations may be performed.

In the sliding mechanism, both atoms have to move away from the surface, thus increasing additively the energy of the transition state. This leads to a bigger energy difference

between the transition and reactant states, or in other words the activation energy for diffusion. On the contrary, for the rolling mechanism, the atoms move in opposite directions. When one atom increases the energy of the resulting state (moving away from the surface, discharging), the other atom decreases this energy (moving toward the surface, charging). As a result, the effects of these two atoms compensate each other, thus leading to a smaller energy difference between transition and reactant states as compared to the sliding mechanism. This makes the rolling mechanism energetically more favorable than the sliding one. Obviously, when the charge transfer is not taken into account, such an energy diagram description is simply not applicable and it is hard to explain preferential rolling motion. It should also be noted that the presented explanation is similar to compensation effects taking place in surface-mounted molecular rotors.⁷⁶ The difference is only in the nature of interactions taking place in corresponding systems.

When the rotation of the fullerene groups is restricted (hence only the hopping mechanism is possible), the energy barriers will be smaller in the case of position-dependent charges as opposed to the fixed charges model. Naturally, although the rolling mechanism of nanocar diffusion is preferred, especially when the charge transfer effects are taken into account, this does not lead to directional motion of nanocars. In the absence of external fields which break the spatial symmetry and add the energy to the system, the number of clockwise and anti-clockwise rotations of the fullerene wheel will on average be equal, in agreement with the second law of thermodynamics.

As it follows from comparison of two main mechanisms (rotation and jumps), the average surface–molecule interaction energy and the average amount of charge transfer should be smaller for diffusion via the hopping mechanism. This is directly observed in our MD calculations for the full-rigid molecules, where the rotation of C_{60} “wheels” is forbidden (Figure 7).

Another important consideration is that for correct calculations of the activation energies the states corresponding to crossing of the saddle point on the potential surface connecting reactant and product states should be sampled with a high statistical weight. Such a transition path determines the true activation barrier for the diffusion. However, if the simulation temperature is low, the highest statistical weight will correspond to saddle points with smallest energies. In chemical kinetics language, it means that we are focusing on the easiest (“elementary”) processes taking place during diffusion. Thus, for the proper calculation of the activation energies for diffusion of the nanocar molecule we used only high temperature data. A similar approach has been used successfully in our previous studies of the crystalline rotors.⁷⁷ The calculated activation energies for completely rigid molecules are much higher as expected: 13.1 ± 2.6 and 20.0 ± 5.4 kcal/mol for Au(111) and Au(100) surfaces correspondingly. This agrees with the analysis of the diffusion mechanisms shown in Figure 10.

4. SUMMARY AND CONCLUSIONS

In this work, we have developed a new theoretical approach for description of charge transfer and chemisorption processes in fullerene–gold systems. The model possesses correct asymptotic properties, which is an important criterion for correct description of the fullerene desorption from the surfaces. This is not the case for the currently used charge-equilibration scheme. The model was developed on the basis of phenomenological observations and simple arguments and

has been parametrized using semiempirical calculations as well as available experimental and theoretical data. The model is computationally more efficient than the existing semiempirical methods, such as the PM6 method, yet it is still quite realistic. It makes this method especially suitable for use in MD simulations of the fullerene-containing compounds on the gold surfaces. Although the present work focused on the gold metal as a surface on which the fullerene adsorption takes place, the method may be extended for other metals or even for nonmetallic substrates.

Most importantly, the model was successfully applied to analyze the dynamics of fullerene and nanocar on the gold surface. Taking into account the charge transfer phenomena results in significantly stronger binding of the fullerene to the surface than it would be if only dispersion interactions are included. As a consequence, the calculated diffusion coefficients are significantly smaller and therefore much closer to experimentally determined values^{6,63} than those reported previously.^{7,8}

Utilizing the energy diagram point of view, we analyzed two different mechanisms of the nanocar’s motion: the sliding and the rolling. We showed, both from the energy point of view and from direct MD simulations, that the rolling mechanism is energetically more favorable than the sliding. This is strongly related to the compensation effect, similar to the one discussed recently as applied to molecular rotors. Such an effect arises because of mutual compensation of the energy change due to the motion of different parts of the molecule. Without dynamic charge transfer being taken into account, such compensation would be negligible, leading to nearly equal probability for sliding and rolling mechanisms. If, however, the charge transfer is included, the difference between these mechanisms becomes more substantial.

In our earlier studies,⁸ we showed that the rigid-body approximation leads to larger diffusion coefficients as compared to all-atomic treatment. However, the qualitative descriptions of adsorbate dynamics obtained with rigid-body and all-atomic MD methods are the same. Thus, the use of the rigid-body approximation in the current work is justified, and it might only affect quantitative results by scaling the dynamical properties such as diffusion coefficients and is unlikely to change qualitative trends.

In conclusion, our charge transfer model consistently explains recent experimental observations on STM manipulations of the nanocars and provides a new theoretical framework for understanding dynamic processes in nano-machines. It will be useful for development of future molecular devices and for further progress in the growing field of nanotechnology.

■ ASSOCIATED CONTENT

S Supporting Information

The derivation of the forces for the charge transfer model. This material is available free of charge via the Internet at <http://pubs.acs.org>.

■ AUTHOR INFORMATION

Corresponding Author

*E-mail: alexey.akimov85@gmail.com.

Notes

The authors declare no competing financial interest.

ACKNOWLEDGMENTS

The authors acknowledge support from the Welch Foundation (Grant C-1559) and from the U.S. National Science Foundation (Grant ECCS-0708765). This work was also supported in part by the Shared University Grid at Rice University funded by U.S. National Science Foundation under Grant EIA-0216467 and a partnership between Rice University, Sun Microsystems, and Sigma Solutions, Inc. C.W. thanks the Rice Quantum Institute REU program and University of Arkansas faculty.

REFERENCES

- (1) Vives, G.; Tour, J. M. *Acc. Chem. Res.* **2009**, *42*, 473–487.
- (2) Shirai, Y.; Morin, J.-F.; Sasaki, T.; Guerrero, J. M.; Tour, J. M. *Chem. Soc. Rev.* **2006**, *35*, 1043–1055.
- (3) Vives, G.; Kang, J.; Kelly, K. F.; Tour, J. M. *Org. Lett.* **2009**, *11*, S602–S605.
- (4) Villagómez, C. J.; Sasaki, T.; Tour, J. M.; Grill, L. *J. Am. Chem. Soc.* **2010**, *72*–191.
- (5) Vives, G.; Tour, J. M. *Tetrahedron Lett.* **2009**, *50*, 1427–1430.
- (6) Shirai, Y.; Osgood, A. J.; Zhao, Y.; Kelly, K. F.; Tour, J. M. *Nano Lett.* **2005**, *5*, 2330–2334.
- (7) Akimov, A. V.; Nemukhin, A. V.; Moskovsky, A. A.; Kolomeisky, A. B.; Tour, J. M. *J. Chem. Theory Comput.* **2008**, *4*, 652–656.
- (8) Konyukhov, S. S.; Kupchenko, I. V.; Moskovsky, A. A.; Nemukhin, A. V.; Akimov, A. V.; Kolomeisky, A. B. *J. Chem. Theory Comput.* **2010**, *6*, 2581–2590.
- (9) Hoogenboom, B. W.; Hesper, R.; Tjeng, L. H.; Sawatzky, G. A. *Phys. Rev. B* **1998**, *57*, 11939–11942.
- (10) Hunt, M. R. C.; Modesti, S.; Rudolf, P.; Palmer, R. E. *Phys. Rev. B* **1995**, *51*, 10039–10047.
- (11) Modesti, S.; Cerasari, S.; Rudolf, P. *Phys. Rev. B* **1993**, *71*, 2469–2472.
- (12) Tsuei, K. D.; Yuh, J. Y.; Tzeng, C. T.; Chu, R. Y.; Chung, S. C.; Tsang, K. L. *Phys. Rev. B* **1997**, *56*, 15412–15420.
- (13) Wang, L.-L.; Cheng, H.-P. *Phys. Rev. B* **2004**, *69*, 045404-1–045404-7.
- (14) Tierney, H. L.; Murphy, C. J.; Jewell, A. D.; Baber, A. E.; Iski, E. V.; Khodaverdian, H. Y.; McGuire, A. F.; Klebanov, N.; Sykes, E. C. H. *Nat. Nanotechnol.* **2011**, *1*–5.
- (15) Harutyunyan, S. R.; Ernst, K. H.; Feringa, B. L. *Nature* **2011**, *479*, 208–211.
- (16) Galli, G. *Comput. Mater. Sci.* **1998**, *12*, 242–258.
- (17) Smith, R.; Webb, R. P. *Proc. R. Soc. Lond. A* **1993**, *441*, 495–499.
- (18) Hobbs, C.; Kantorovich, L. *Nanotechnology* **2004**, *15*, S1–S4.
- (19) Henry, D. J.; Evans, E.; Yarovsky, I. *J. Phys. Chem. B* **2006**, *110*, 15963–15972.
- (20) Bubnis, G. J.; Mayne, H. R. *J. Phys. Chem. C* **2010**, *114*, 13071–13082.
- (21) Tzeng, C. T.; Lo, W. S.; Yuh, J. Y.; Chu, R. Y.; Tsuei, K. D. *Phys. Rev. B* **2000**, *61*, 2263–2272.
- (22) Maxwell, A. J.; Bruhwiler, P. A.; Nilsson, A.; Martensson, N. *Phys. Rev. B* **1994**, *49*, 10717–10725.
- (23) Baxter, R. J.; Teobaldi, G.; Zerbetto, F. *Langmuir* **2003**, *19*, 7335–7340.
- (24) Sau, J.; Neaton, J.; Choi, H.; Louie, S.; Cohen, M. *Phys. Rev. Lett.* **2008**, *101*, 026804.
- (25) Li, H.; Pussi, K.; Hanna, K.; Wang, L.-L.; Johnson, D.; Cheng, H.-P.; Shin, H.; Curtarolo, S.; Moritz, W.; Smerdon, J.; McGrath, R.; Diehl, R. *Phys. Rev. Lett.* **2009**, *103*, 056101–1–4.
- (26) Cepek, C.; Goldoni, A.; Modesti, S. *Phys. Rev. B* **1996**, *53*, 7466–7472.
- (27) Stengel, M.; Vita, A.; Baldereschi, A. *Phys. Rev. Lett.* **2003**, *91*, 166101–1–166106–4.
- (28) Weckesser, J.; Cepek, C.; Fasel, R.; Barth, J. V.; Baumberger, F.; Greber, T.; Kern, K. *J. Chem. Phys.* **2001**, *115*, 9001.
- (29) Shukla, M. K.; Dubey, M.; Leszczynski, J. *ACS Nano* **2008**, *2*, 227–234.
- (30) Zhu, X.-Y.; Dutton, G.; Quinn, D.; Lindstrom, C.; Schultz, N.; Truhlar, D. *Phys. Rev. B* **2006**, *74*, 241401(R).
- (31) Rappe, A. K.; Goddard, W. A. *J. Phys. Chem.* **1991**, *95*, 3358–3363.
- (32) Kitao, O.; Ogawa, T. *Mol. Phys.* **2003**, *101*, 3–17.
- (33) Oda, A.; Hiroto, S. *J. Mol. Struct.: THEOCHEM* **2003**, *634*, 159–170.
- (34) Zhang, M.; Fournier, R. *J. Phys. Chem. A* **2009**, *113*, 3162–3170.
- (35) Sevcik, J.; Demiralp, E.; Cagin, T.; Goddard, W. A. *J. Comput. Chem.* **2002**, *23*, 1507–1514.
- (36) Chen, J.; Martinez, T. *J. Chem. Phys. Lett.* **2007**, *438*, 315–320.
- (37) Jalkanen, J.-P.; Zerbetto, F. *J. Phys. Chem. B* **2006**, *110*, 5595–5601.
- (38) Mendoza, S. M.; Whelan, C. M.; Jalkanen, J.-P.; Zerbetto, F.; Gatti, F. G.; Kay, E. R.; Leigh, D. A.; Lubomska, M.; Rudolf, P. *J. Chem. Phys.* **2005**, *123*, 244708-1–244708-7.
- (39) Baxter, R. J.; Rudolf, P.; Teobaldi, G.; Zerbetto, F. *ChemPhysChem* **2004**, *5*, 245–248.
- (40) Teobaldi, G.; Zerbetto, F. *Small* **2007**, *3*, 1694–1698.
- (41) Stewart, J. J. *J. P. J. Mol. Model.* **2007**, *13*, 1173–1213.
- (42) Wang, L.-L.; Cheng, H.-P. *Phys. Rev. B* **2004**, *69*, 165417.
- (43) Simonetta, M. *Int. J. Quantum Chem.* **1986**, *29*, 1555–1560.
- (44) Simonetta, M.; Gavezzotti, A. *J. Mol. Struct.* **1984**, *107*, 75–86.
- (45) Zilberman, I.; Pelmenschikov, A.; McGrath, C. J.; Davis, W.; Leszczynska, D.; Leszczynski, J. *Int. J. Mol. Sci.* **2002**, *3*, 801–813.
- (46) Hoffmann, R. *J. Chem. Phys.* **1963**, *39*, 1397.
- (47) Hoffmann, R. *J. Chem. Phys.* **1964**, *40*, 2745.
- (48) Hoffmann, R. *J. Chem. Phys.* **1964**, *40*, 2474.
- (49) Hoffmann, R. *J. Chem. Phys.* **1964**, *40*, 2480.
- (50) Pyykkö, P.; Lohr, L. L., Jr. *Inorg. Chem.* **1981**, *20*, 1950–1959.
- (51) Pyykkö, P.; Laaksonen, L. *J. Phys. Chem.* **1984**, *88*, 4892–4895.
- (52) Fitzpatrick, N. J.; Murphy, G. H. *Inorg. Chim. Acta* **1986**, *111*, 139–140.
- (53) Frisch, M. J.; et al. *Gaussian 03*, revision D.01 (see the Supporting Information for full citation).
- (54) Rappe, A. K.; Casewit, C. J.; Colwell, K. S.; Goddard III, W. A.; Skiff, W. M. *J. Am. Chem. Soc.* **1992**, *114*, 10024–10035.
- (55) Lewis, L. J.; Jensen, P.; Combe, N.; Barrat, J. L. *Phys. Rev. B* **2000**, *61*, 16084–16090.
- (56) Arcidiacono, S.; Walther, J.; Poulikakos, D.; Passerone, D.; Kourmoutsakos, P. *Phys. Rev. Lett.* **2005**, *94*, 105502-1–105502-4.
- (57) Luedtke, W. D.; Landman, U. *Phys. Rev. Lett.* **1999**, *82*, 3835–3838.
- (58) Luedtke, W. D.; Landman, U. *J. Phys. Chem.* **1996**, *100*, 13323–13329.
- (59) Kamberaj, H.; Low, R. J.; Neal, M. P. *J. Chem. Phys.* **2005**, *122*, 224114-1–224114-30.
- (60) Shustorovich, E. *Acc. Chem. Res.* **1988**, *21*, 183–189.
- (61) Shustorovich, E. *Surf. Sci.* **1985**, *163*, 645–654.
- (62) Shustorovich, E. M. *Surf. Sci. Lett.* **1985**, *150*, L115–L121.
- (63) Khatua, S.; Godoy, J.; Tour, J. M.; Link, S. *J. Phys. Chem. Lett.* **2010**, *1*, 3288–3291.
- (64) Clayton, K.; Khatua, S.; Guerrero, J. M.; Tcherniak, A.; Tour, J. M.; Link, S. *J. Chem. Phys.* **2009**, *130*, 164710-1–164710-9.
- (65) Khatua, S.; Guerrero, J. M.; Clayton, K.; Vives, G.; Kolomeisky, A. B.; Tour, J. M.; Link, S. *ACS Nano* **2009**, *3*, 351–356.
- (66) Armstrong, J. A.; Chakravarty, C.; Ballone, P. *J. Chem. Phys.* **2012**, *136*, 124503.
- (67) Lyubimov, I.; Guenza, M. *Phys. Rev. E* **2011**, *84*, 031801.
- (68) Lyubimov, I. Y.; McCarty, J.; Clark, A.; Guenza, M. G. *J. Chem. Phys.* **2010**, *132*, 224903.
- (69) Rosenfeld, Y. *Phys. Rev. A* **1977**, *15*, 2545–2549.
- (70) Gomer, R. *Rep. Prog. Phys.* **1990**, *53*, 917.
- (71) Ehrlich, G.; Stolt, K. *Annu. Rev. Phys. Chem.* **1980**, *31*, 603–637.
- (72) Brand, J. L.; Arena, M. V.; Deckert, A. A.; George, S. M. *J. Chem. Phys.* **1990**, *92*, 5136–5143.
- (73) Cohen, D.; Zeiri, Y. *J. Chem. Phys.* **1992**, *97*, 1531–1541.

- (74) Zeiri, Y. *Can. J. Chem.* **1994**, *72*, 813–820.
- (75) Arena, M.; Deckert, A.; Brand, J.; George, S. *J. Phys. Chem.* **1990**, *94*, 6792–6797.
- (76) Akimov, A.; Kolomeisky, A. B. *J. Phys. Chem. C* **2011**, *115*, 125–131.
- (77) Akimov, A. V.; Kolomeisky, A. B. *J. Phys. Chem. C* **2011**, *115*, 13584–13591.